IAEA
International Atomic Energy Agency

20th IAEA Fusion Energy Conference
Vilamoura, Portugal, 1 to 6 November 2004

IAEA-CN-116/EX/P5-11

THE ROLE OF SHAPING IN THE SAWTOOTH INSTABLITY

E.A. LAZARUS,[1] F.L. WAELBROECK,[2] M.E. AUSTIN,[2] K.H. BURRELL, J.R. FERRON, A.W. HYATT, T.C. LUCE, T.H. OSBORNE, M.S. CHU, P. GOHIL, R.J. GOEBNER, W.W. HEIDBRINK,[3] C.L. HSIEH, R.J. JAYAKUMAR,[4] L.L. LAO, J. LOHR, M.A. MAKOWSKI,[4] C.C. PETTY, P.A. POLITZER, R. PRATER, H. REIMERDES,[5] T.L. RHODES,[6] J.T. SCOVILLE, E.J. STRAIT, A.D. TURNBULL, M.R. WADE,[1] and C. ZHANG[7]

General Atomics
San Diego, California 92186-5608
United States of America

[1]Oak Ridge National Laboratory, Oak Ridge, Tennessee, USA
[2]University of Texas, Austin, Texas, USA
[3]University of California-Irvine, Irvine, California, USA
[4]Lawrence Livermore National Laboratory, Livermore, California, USA
[5]Columbia University, New York, New York, USA
[6]University of California-Los Angeles, Los Angeles, California, USA
[7]ASIPP, China.

The Role of Shaping in the Sawtooth Instability

E.A. Lazarus,[1] F.L. Waelbroeck,[2] M.E. Austin,[2] K.H. Burrell,[3] J.R. Ferron,[3] A.W. Hyatt,[3] T.C. Luce,[3] T.H. Osborne,[3] M.S. Chu,[3] P. Gohil,[3] R.J. Groebner,[3] W.W. Heidbrink,[4] C.L. Hsieh,[3] R.J. Jayakumar,[5] L.L. Lao,[3] J. Lohr,[3] M.A. Makowski,[5] C.C. Petty,[3] P.A. Politzer,[3] R. Prater,[3] H. Reimerdes,[6] T.L. Rhodes,[7] J.T. Scoville,[3] E.J. Strait,[3] A.D. Turnbull,[3] M.R. Wade,[1] G. Wang,[7]and C. Zhang[8]

[1]Oak Ridge National Laboratory, Oak Ridge, Tennessee, USA
[2]University of Texas at Austin, Austin, Texas, USA
[3]General Atomics, P.O. Box 85608, San Diego, California 92186-5608, USA
[4]University of California-Irvine, Irvine, California, USA
[5]Lawrence Livermore National Laboratory, Livermore, California, USA
[6]Columbia University, New York, New York, USA
[7]University of California-Los Angeles, Los Angeles, California, USA
[8]ASIPP,China

e-mail contact of main author: lazarus@fusion.gat.com

Abstract. We report on experiments that attempt to clarify the role of interchange and internal kink modes in the sawtooth oscillations by comparing bean- and oval-shaped plasmas. We find that differences in the transport processes during the sawtooth ramp play an important role in determining the nature of the oscillations. For both shapes the crash flattens the q profile and returns q_0 to unity. A key difference between the two shapes, however, is that in the bean the safety factor rapidly drops below unity during the subsequent ramp while in the oval it remains very close to unity. As a result of this, a saturated quasi-interchange mode develops fairly early and grows steadily during the ramp of oval discharges. The crash appears to be triggered by a secondary instability that locks to the saturated quasi-interchange mode. In the bean, by contrast, the crash is consistent with a rapid reconnection process. FIR interferometry shows that the oval exhibits significant turbulence in the electron channel, consistent with the observation of large electron heat diffusivities. This is supported by examination of the impulse response to central ECH. The ion transport, however, is approximately neoclassical. In the bean, by contrast, the electron temperature rises steadily, while T_i first saturates and then decreases during the last quarter of the ramp.

1. Introduction

We have performed experiments intended to separate the roles of interchange and internal kink stability in the sawtooth. This is accomplished by changing the plasma shape. We find significant differences in both the evolution within a sawtooth period and in the nature of the sawtooth crash itself. In this paper we will detail these differences. In an oval-shaped plasma with simple monotonic pressure and q profiles, the Mercier criterion will be violated while q_0 is somewhat above 1. The destabilizing terms are elongation, κ, and beta poloidal, β_p, whereas triangularity, δ, is stabilizing. If we make a low-κ bean shape, for similar profiles the Mercier criterion can be satisfied for q_0 somewhat below 1. Of course the stability criterion for the resistive internal kink remains q=1 in both cases. This paper is organized as follows. In Sec. 2 we discuss the experimental conditions and global behavior. Section 3 focuses on the evolution during the sawtooth crash. Section 4 presents results for the sawtooth ramp. We summarize the results in Sec. 5 and present a concluding discussion in Sec. 6. This experiment has been in progress for some years. We have found the principal features to be the same on a year-to-year comparison. The primary differences have been in improved diagnostic capabilities in DIII-D that have led to a better understanding of the experiment.

2. Experimental Conditions

The oval and bean shapes satisfy a number of conditions we established for this experiment. The first and most important condition is to maximize the contrast in interchange stability. That is, we choose shapes that show substantial difference in magnetic well in the center of the discharge (Fig. 1), where it is seen we actually have a magnetic hill in the central region of the oval plasma. A second condition we impose is that both shapes can be made without reconfiguring the poloidal field power supplies. This allows us to switch between

the shapes on a shot-by-shot basis, minimizing the effects of systematic differences in the tokamak conditions and in the diagnostics. A third condition was that we wanted to study the L-mode plasma, the simplest situation and lowest β_P readily achievable. The remainder of the plasma conditions is largely set by diagnostic requirements. The single neutral beam is required for motional Stark effect (MSE) and CER diagnostics. The low density allows for good penetration of this beam to the center of the plasma, and avoids H-mode in the bean shape. B_T determines the spatial range of the ECE diagnostic.

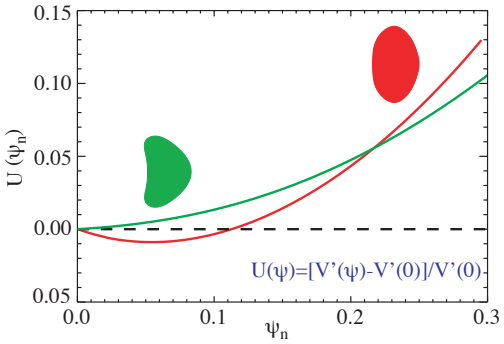

Fig. 1. The magnetic well parameter in the central region of the plasma for the two shapes.

The typical discharge evolution is shown in Fig. 2. The plasmas are always created using an early (500 ms) beam, as low density is desirable for reasons of measurement and we wanted to avoid any locked-mode issues. The startup is robust in that we always get the same type of sawteeth. The plasma current is chosen so the sawtooth inversion radius, r_i, is not too large and we get several ECE channels outside r_i. The confinement is comparable in the two shapes, leading to similar stored energy and edge safety factor. Although the bean is limited, the separatrix is close to the plasma boundary and we think q_{95} is more comparable than q_{lim}. $q_{Mercier}$ in Fig. 2 is an axial approximation of the q value required to satisfy the Mercier criterion and they differ as expected. The internal inductivity, l_i, also varies with the plasma shape. The neutral beam required for MSE and CER is turned on at 1700 ms. Data is mostly taken in the interval 2500-4500 ms. At that time, aside from the sawtooth effects, the plasma current is fully equilibrated as evidenced by the constancy of the mean MSE signals.

The boundary shapes are shown in Fig. 3. The inner contour corresponds to the inversion radius. We take this opportunity to show the location of the critical diagnostics. These particular equilibria are detailed further in Table I. Here we show parameters for the two levels of plasma current used for each shape.

Several differences are immediately apparent in the 2 shapes. The plasmas have similar confinement times of $\tau_E \approx$ 100 ms. Within a discharge the sawtooth is very reproducible. The sawtooth period, τ_s, is about 100 ms in the bean and 50 ms in the oval. Both have a relaxation event at 1/4-1/3 the sawtooth period. The oval has a large precursor oscillation before the crash. The bean has no precursor oscillation but does have a large post-

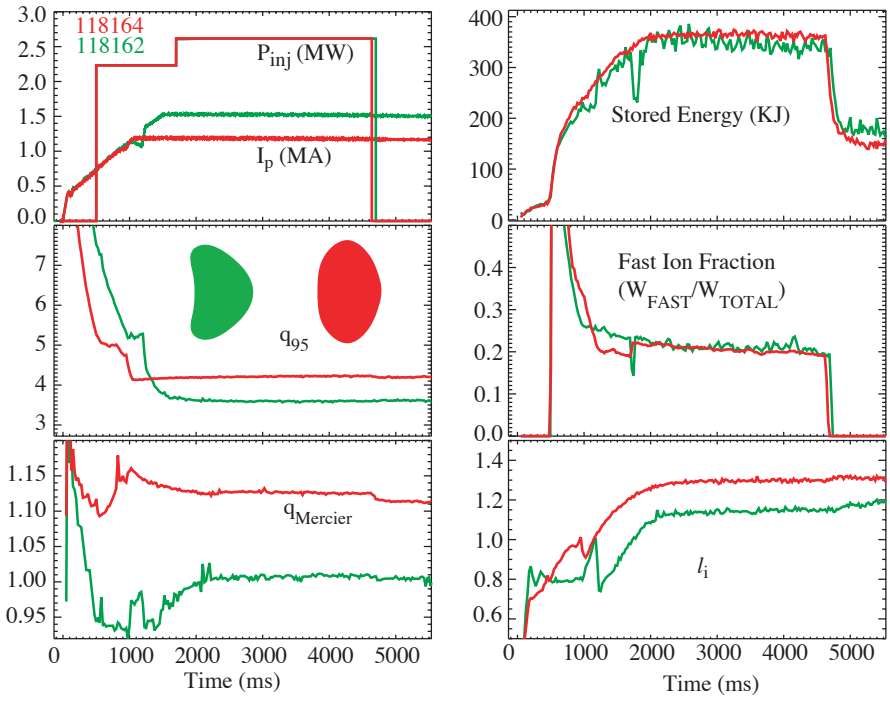

Fig. 2. The typical evolution of a discharge in this experiment. Shown are plasma current and neutral beam power, the plasma stored energy, safety factor, fast ion fraction, an approximate value of q_0 required to satisfy the Mercier criterion, and internal inductivity, l_i.

TABLE I. Selected Parameters

	Bean 1	Bean 2	Oval 1	Oval 2
Shot	113920	118162	113915	118164
I_p (MA)	1.38	1.52	0.88	1.18
B_T (T)	1.79	1.85	1.80	1.85
V (m^3)	17.5	17.6	20.1	20.1
$\langle n_e \rangle$ (x10^{19} m^3)	2.0	2.5	1.9	2.75
β_p	0.22	0.24	0.45	0.38
β_{p1} (Bussac)	0.16	0.19	0.41	0.33
l_i	1.24	1.15	1.41	1.29
W^{MHD} (MJ)	0.25	0.34	0.24	0.37
τ_E^* (ms), τ_E^{th} (ms)	93	127, 75	90	140, 75
τ_s (ms)	90	154	59	80
q_{95}	3.9	3.6	5.4	4.2
r_i (normalized inversion radius)	0.38	0.44	0.28	0.35
W^{fast}/W^{MHD}	0.27	0.13	0.25	0.11
Reconnection δB_θ (G)	219	293	85	129

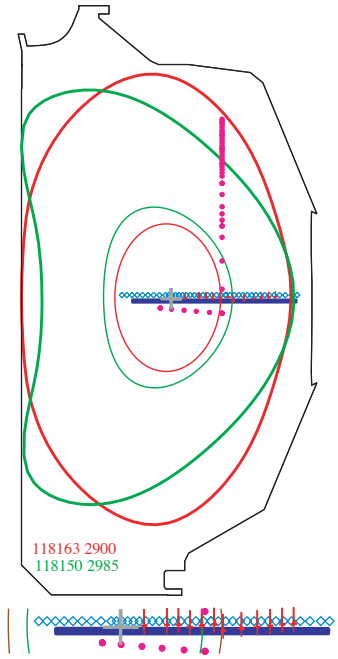

Fig. 3. Plasma boundary shapes for bean and oval plasmas. The inner surfaces are at the location of r_i. Diagnostic (in an expanded view below) locations are shown. The magenta solid circles are Thomson scattering (n_e, T_e). The upside-down red daggers are CER (T_i) locations. The blue bar is the MSE (B_Z/B_T) range of locations. The blue diamonds are ECE (T_e) locations, displaced from Z=0 for clarity. The large grey + is the magnetic axis for both.

cursor oscillation, that is, it crashes from a near-axisymmetric condition into a helical state. The crash time is about 40 μs in the bean. In the oval, the crash time is longer and not as clearly defined. This is discussed in more detail in the next section. In the bean, the crash is an identifiable event in the raw MSE signals ($\tan^{-1}$ [$B_Z(t)/B_T$]) but this is not true in the oval. The crash amplitude, (T_e^{max} - T_e^{min})/T_e^{min} is much larger in the bean than in the oval. The sawtooth crash in the bean is a violent event, and about 15% of the stored energy leaves the plasma. In the oval the sawtooth crash is benign and there is no net energy loss from the plasma. While fast-ions from NBI appear to provide some stabilization and extension of the sawtooth period, changes in the fast ion fraction, say by replacing part of the neutral beam power with ECH, do not change this qualitative behavior. The sawtooth periods are reduced in both cases by ~20%, but the features discussed in this paper are not changed. The δB_θ in Table I is obtained from the MSE channel showing the biggest excursion by averaging over several sawteeth. While in the case of the bean, this is an accurate portrayal of the change at the crash time, in the case of the oval the crash is not as well defined and we are simply asserting that this is the magnitude of the change but it may be occurring over a few ms.

3. The Sawtooth Crash

We will begin this discussion by displaying a color map of the crash as seen in the ECE diagnostic (Fig. 4). In the bean we see no structure prior to the crash. From all the available data, the bean plasma prior to the crash is exceedingly axisymmetric. After the crash there are n=1 oscillations and a double island structure is observed. The identification of islands is confirmed by a cross-correlation analysis of the ECE with the n=1 signal seen on magnetic probes. This shows phases jumps consistent with a double island structure (Fig. 5, upper panel).

In the oval, the precursor oscillations are reflected in the ECE signals, as seen in Fig. 4(b). The features of importance here are the sustained period of oscillation before 3434.5 ms, the interval from 3434.5 to 3434.75, and the final few oscillations after 3534.75 leading to a crash. These are generic features of the sawtooth collapse in the oval.

The correlation analysis is shown in the lower panel of Fig. 5. What is interesting here is the single phase jump on the inboard side. If we were observing an island there would be an opposite phase jump on the low field side where there is no sign of such a jump. The only

way to produce this phase jump on the high field side is to combine the m=1 and m=2 components of an ideal quasi-interchange mode [1]. If the m=1 component is kink-like the phase shift will disappear. If there is an island there will be a corresponding phase shift on the other side of the axis. Prior to the interval 3434.5 to 3434.75 in Fig. 6(b) there is another n=1 at higher frequency than the primary mode. This mode bursts and chirps down in frequency, reoccurring about every 5 ms. The last burst appears to chirp all the way down to the primary n=1 frequency and lock to it. This apparent locking always occurs in the oval sawteeth and precedes the crash by a few oscillations. Notice that the modulation depth of the primary n=1 is deeper after this event. If we take those last few cycles of oscillation the correlation analysis is less reliable but still shows the same single phase jump. Thus there is no evidence of tearing prior to the crash. The final stages of the oval crash are shown in more detail in Fig. 6. We show an outer magnetic loop that illustrates the growing precursor leading up to the crash at 3435.19 ms. At, and prior to t_c - 1130 μs, the helical deformation in the temperature is just visible in the T_e profile. The deformation continues to grow until the hot spot vanishes. It is quite plausible to describe this as a helical deformation as late as t_c - 420 μs where the gradient remains negative. At t_c - 90 μs where most of the profile has crashed there may be an island but we have no direct evidence.

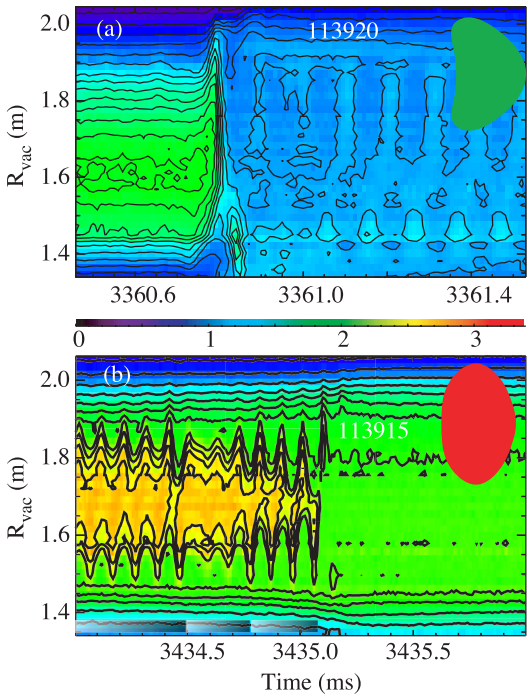

Fig. 4. The evolution of a sawtooth crash as a color map of T_e vs. R_{vac} and time; (a) bean shape and (b) the oval shape. R_{vac} is the radius an ECE channel would have in the vacuum field (B_θ=0).

We contrast this to the behavior in the bean where there is only a slight flattening of the temperature profile in a narrow region and the first sign of the instability in the T_e profile occurs 40 μs before the crash. The profile simply collapses from the low field side. In the bean it is straightforward to identify a crash time as the time for the hot spot to vanish from the core; this is 40 μs. In the oval, if we apply the same definition the crash time is ~70 μs. However, if we were to look at a central ECE channel to define a crash time in the oval this would be ≈1300 μs, If we were to take the locking of n=1 modes as the beginning of the crash we would get a value of 600 μs. There is no clear definition, but it is slower than in the bean.

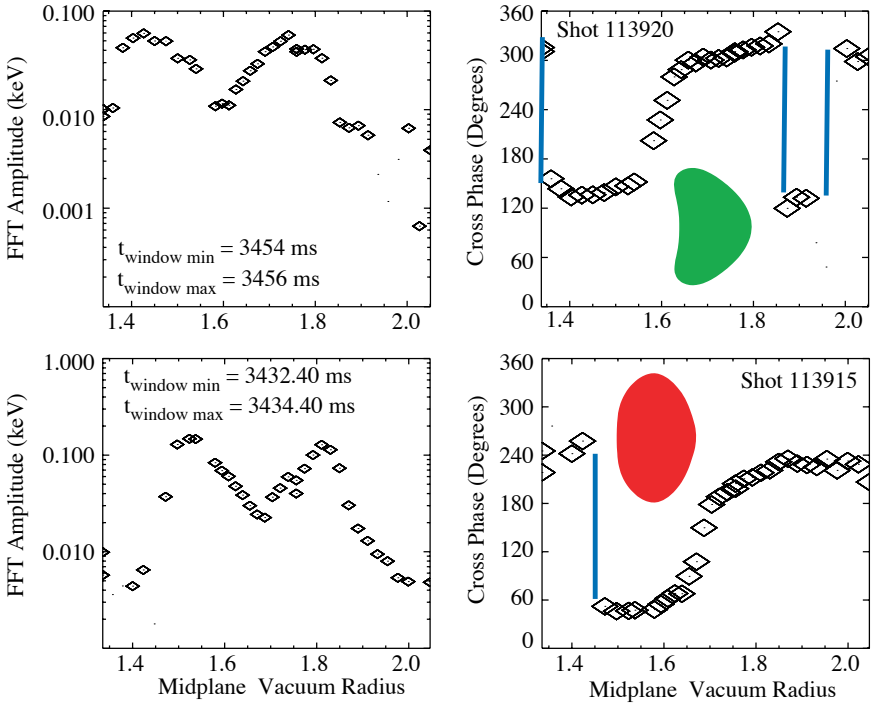

Fig. 5. FFT of ECE corrrelation with n=1 magnetic signal..

4. Evolution During the Ramp

4.1. Equilibrium

The evolution of the plasma between sawteeth is markedly different in the bean and oval. We begin with equilibria. Our analysis differs somewhat from the usual application of EFIT in that we do not attempt to calculate the total pressure based on one equilibrium solution and use this $p(\psi)$ in a subsequent iteration. Instead,within a single equilibrium calculation we use the ECE signals (T_e) as a constraint on the flux surface geometry along with the MSE. We do use the measured pressure outside ρ=0.7 where we expect fast ion pressure to be nil.

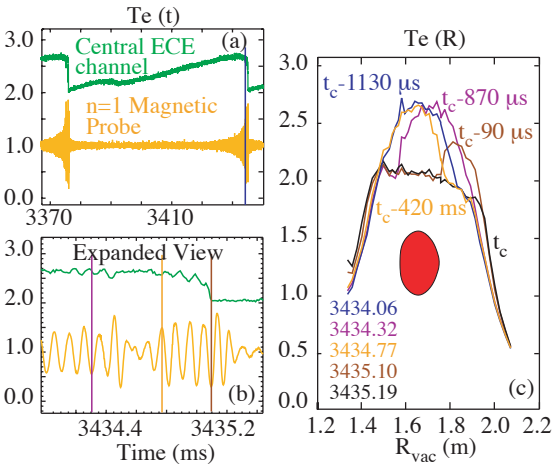

Fig. 6. The evolution of the sawtooth crash in an oval; (a) dB_θ/dt from an outer midplane probe and a central ECE channel vs. time, (b) expanded view of (a), and (c) the evolution of the T_e profile from ECE. t_c is the crash time and R_{vac} is the vacuum field radius of the ECE array.

The results for the oval and bean are shown in Figs. 7 and 8. In the oval, the sawtooth is a minor event with minimal change in the safety factor or pressure profile. We should remark that in ovals at higher current q remains flat (Fig. 7) but q_{min} does drop distinctly below unity during the sawtooth cycle. The bean is an entirely different matter with significant changes in both profiles. Note that the lowest q_0 does not occur at the latest time before the crash, but does seem to occur when a maximum p_0 is reached. This is related to the ion behavior discussed below. The hollow pressure profile at the earliest time in the bean cannot be confirmed from the kinetic data, as the density profile remains too uncertain.

4.2. Ion Behavior

In Fig. 9 we show the ion temperature relative to the electron temperature for bean and oval plasmas. The differences shown are characteristics of the shaping, always seen in comparisons of beans and ovals.

In the oval, the ion sawtooth is much larger than the electron sawtooth but continues an approximately linear ramp, as do the electrons. In the bean, at ~60% of the sawtooth period the ion temperature (and toroidal rotation velocity) roll over and begin decreasing. Also, $\partial T_e/\partial t$ is reduced at that time. In both cases the neutral beam power is shared near equally between ions and electrons. In this oval plasma we see more correlation of MSE (B_θ) with the crash than was observed at lower plasma current (Table I, Oval1 vs. Oval2).

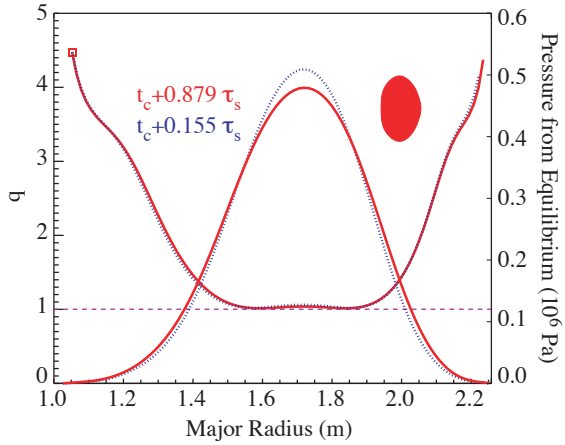

Fig. 7. The evolution of pressure and safety factor in an oval. t_c is the crash time.

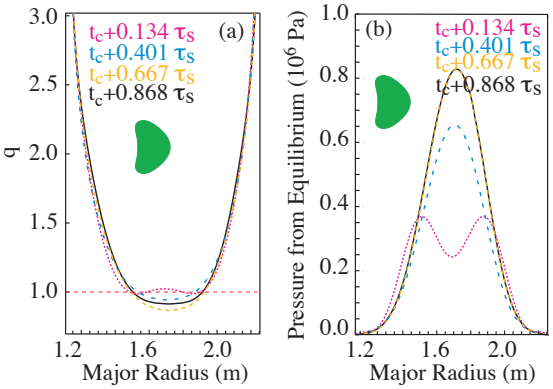

Fig. 8. The evolution of pressure and safety factor in a bean. Times are expressed as fractions of a sawtooth period. t_c is the crash time. At the time t_c + 0.134•τ_s the q-profile does cross q=1 twice, consistent with the correlation analysis showing a double island structure.

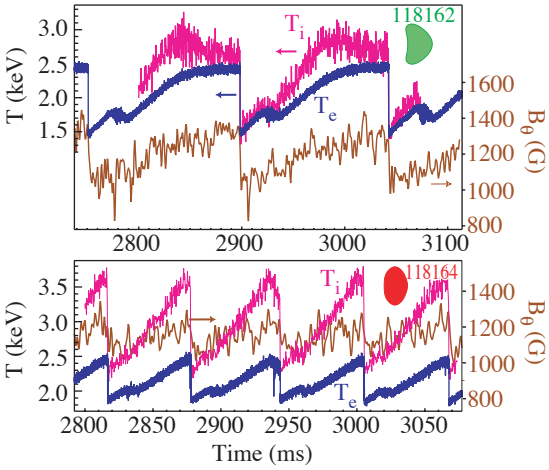

Fig. 9. T_i from the innermost CER channel, T_e from a nearby ECE channel and B_θ from an MSE channel. All are at $\rho \approx 0.1$ and the MSE signal is smoothed (1 ms). (a) The bean shape and (b) an oval plasma.

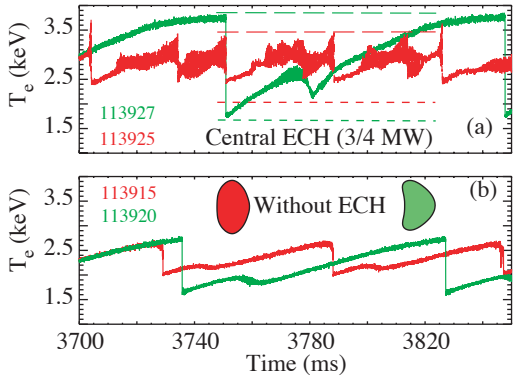

Fig. 10. The response of the oval and bean plasmas to central electron cyclotron heating. (a) shows ECE signals near the axis, but outside the deposition region, with ECH and is to be compared with (b) a similar shot without ECH. In (a), the long dashed lines are simply a reference to peak values. The short dashed lines correspond to the foot of the sawteeth prior to turning on the ECH. (Oval traces are red, bean traces are green.)

4.3. Response to Central ECH

The *q*-profiles motivated an examination of the electron response to ECH deposited near the axis ($\rho \approx 0.07$). In Fig. 10 we show the response to sustained central ECH after the plasma has equilibrated. In the bean case, the sawteeth simply become larger.

In the oval the response is more complicated; the sawtooth interval is dominated by the m/n=1/1 mode, the sawtooth period becomes irregular, and the baseline of the sawtooth is raised considerably. Note that the sawtooth period is longer in those sawteeth with more violent partial reconnections. This behavior, along with the shearless central region of the oval motivated us to look at the impulse response (Fig. 11). The bean responds; the oval does not.

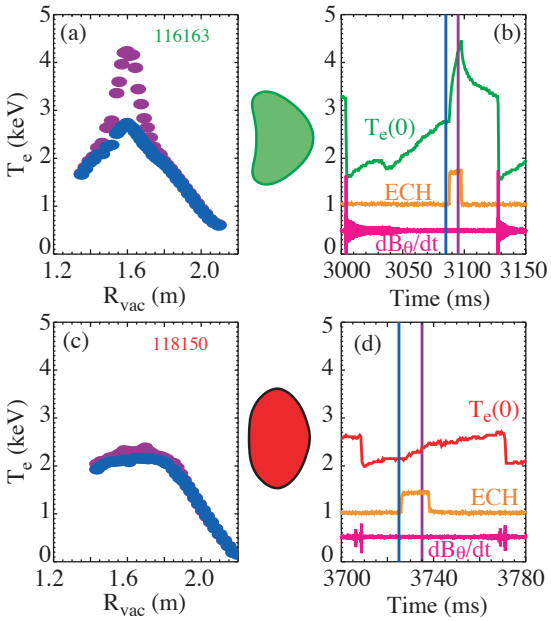

Fig. 11. The impulse response to ECH. (a) and (c) are the T_e profiles at the times indicated in (b) and (d). In (b) and (d) the dB_θ/dt signal from an outer midplane detector and the ECH pulse are shown along with the central T_e. $d\beta_\theta/dt$ (a.u.) signal is also offset. The ECH power baseline is offset by 1 MW. dB_θ/dt (a.u.) is also offset.

4.4. Transport Analysis

We have analyzed the transport coefficients for 2 cases without ECH. The analysis is done with TRANSP and markers at the sawtooth crashes are used to allow discontinuous behavior. Averaging over sawteeth was necessary to smooth noise in the grid motion from the equilibria computed every 5 ms. Since we needed to smooth the equilibria, we thought it necessary to also smooth all the data in the same way. The smoothing technique is to shift all data onto a time base as a fraction of sawtooth period and do a best fit, either linear or parabolic, as seemed most suitable. In Fig. 12 we show diffusivities volume-averaged from the axis to ρ=0.3. Times that showed the effects of the switching transient are not shown. There are two very dramatic results: χ_e is vastly different in the two shapes, and is very large in the oval. This is consistent with the ECH response seen in Fig. 11. Also, in the oval where ion sawteeth are much larger than electron sawteeth, the ion diffusivity is quite near the neoclassical level. The diffusivities in the bean are more typical of the core of a tokamak plasma. Although we have not obtained the data

necessary to do satisfactory transport analysis for cases with the ECH pulse, in the oval, the power deposited to electrons within ρ=0.25 is increased over the cases discussed here by a factor of 25 with no commensurate increase in ∇T_e. We can conclude that χ_e in the plasma center is enormous.

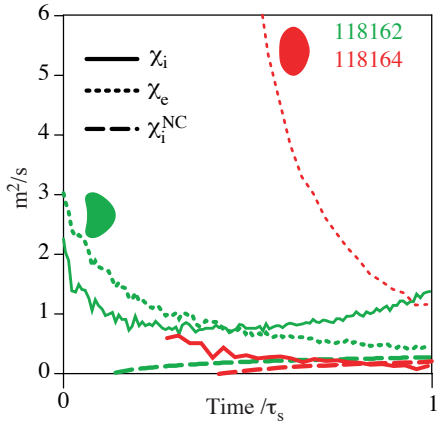

Fig. 12. Calculated thermal diffusivities, volume-averaged from the axis to ρ=0.3, in the two shapes.

5. Summary of Results

We summarize the experimental observations, although space limitations in these proceedings have not allowed us to discuss all the observations in detail. While both the bean and oval exhibit sawtooth waveforms, the behaviors are radically different.

1. The bean crash occurs on an ideal time scale with no precursor oscillations. The nature of the oval crash is uncertain, but we see ideal behavior (no tearing) to within 100 μs or so of the crash. The possibility that the final stage is a resistive interchange-driven Taylor relaxation cannot be ruled out at this time. The bean crash expels energy beyond the last closed flux surface, while the oval does not.
2. Both exhibit a relaxation event at about 25% of the sawtooth period. While both collapse to an equilibrium state with a large region of $q \approx 1$, the bean manages to develop magnetic shear after the relaxation event and improved electron confinement. Prior to this relaxation event the electron response to an ECH pulse is similar to that of the oval. Recovery from the relaxation event is seen earlier in the ions than in the electrons in the bean. In the oval, the relaxation event is barely observed in T_i, while it remains quite clear in T_e. To within the 274 μs resolution in T_i, the crash is simultaneous with T_e.
3. While the oval exhibits a limited central ∇T_e, there is not a similar limitation to ∇T_i. From TRANSP analysis about half the beam power is deposited in each channel in both cases. The same is true within ρ=0.3, so the transport rates differ considerably.
4. In the oval, the ion sawtooth amplitude is much larger than the electron sawtooth while in the bean they are comparable and the ion evolution exhibits a more complex behavior (rollover).
5. An examination of the cross-correlation of T_e fluctuations shows that the m/n=1/1 oscillation is always present in the core in the oval. It may not be present at the level that creates a macroscopic distortion, but there appears to always be a helical magnetic axis. This is not true in the bean, which appears to be axisymmetric even at the level of the microscopic T_e fluctuations. The spectrum of density fluctuations is broader for the oval for intermediate k vectors. For low k, the observed difference only appears to reside in the observation of the m/n=1/1 mode and its higher harmonics.
6. There appear to be some differences in the oval with increasing plasma current such as lower q_{min} and more of a signature of reconnection (Fig. 8) than was seen at lower current, as is reflected in the δB_θ values seen in Table I. It is possible that as q_{95} is lowered, the kink mode is playing a stronger role in the oval. However, the FFT of the ECE retains the single phase shift signature of a quasi-interchange. In the bean we do not see evidence of an important change with plasma current.

6. Discussion

At this time the analysis of the experiment is still in progress. We set out to change the magnetic well, and were successful. The resulting plasmas have very different behaviors. Of course, this does not mean the differences are attributable to the change in magnetic well. We believe the correlation analysis of the n=1 component of the ECE signals identifies the instability in the oval as quasi-interchange. Conversely, the lack of such an inboard phase jump in the bean prior to the crash implies the eigenfunction is kink-like.

An important motivation for the experiment was to test a suggestion [2] that some sawtooth crashes might be more accurately described as Taylor relaxation events than by complete reconnection as in the Kadomtsev model. Gimblett's relaxation model was itself motivated by the desire to account for observations of sawteeth in which the central q remained below unity at all times, in flagrant violation of the Kadomtsev model. We expected that Taylor relaxation would be favored over Kadomtsev reconnection in the oval due to the destabilization of ideal and resistive interchange modes by the unfavorable curvature. The observations reported here, however, show that in DIII-D the central q does return to unity after every crash, thereby removing one of the motivations for the Taylor relaxation model. Nevertheless, the idea that magnetic turbulence plays a role is supported in part by the combined observations in the oval of a very intense and broad spectrum of fluctuations, an exceptionally high electron thermal diffusivity, and the absence of the current profile peaking after the crash.

An important feature of the oval is the presence of a saturated n=1 mode. This mode may correspond to the saturation of the quasi-interchange predicted by Waelbroeck [3]. This saturation explains the continuation of the ramp long after the ideal MHD threshold has been crossed. In the bean, by contrast, stability seems to be provided by the diamagnetic rotation associated with the steep pressure gradients. The sawteeth in the bean and oval are both qualitatively consistent with the Kadomtsev model, although in the bean the model must be modified to account for the stabilizing effects of diamagnetic rotation and for the acceleration of the reconnection rate due to two-fluid effects [4,5]. We have seen no evidence of the secondary ballooning mode activity at intermediate n predicted by Bussac and observed on TFTR [6,7], but have not yet ruled out the possibility that such modes may play a role.

A picture of interchange instability flattening the plasma pressure profile in the oval during the sawtooth ramp is not supported by the experiment. The density profile is less certain than other quantities. Nevertheless, we do not believe the uncertainty is sufficient to allow a hollow density profile to compensate the ion temperature gradient. Thus, we believe central ∇p is negative during the sawtooth ramp in the oval. Inclusion of the fast ion pressure makes ∇p still more negative. In fact, ideal stability offers little understanding as the plasmas are calculated to be ideally unstable throughout the sawtooth interval. The difference of a factor of 2 in τ_s is unexplained. We have looked for a signature of low-k resistive interchange driven turbulence and not found one. We see a difference in density fluctuation spectra (Fig. 13) at larger k and higher frequencies where $k_\theta \rho_i \sim$ 2-3 may be indicative of trapped electron modes. This would be consistent with the observation that the turbulence is seen in the electron channel while ion confinement is excellent in the oval.

If we try to look at the applicability of these results to burning plasma, two features are of potential interest. First, in the case of strong shaping the violent nature of the sawtooth collapse, with ≈15% of the energy expelled from the plasma, may be cause for concern. Second, in conditions where the ion heating is via electrons through the exchange term, the inability to peak T_e in the core will be reflected directly in the T_i profile, if the shaping is weak.

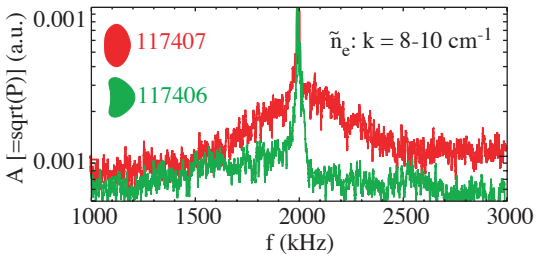

Fig. 13. The spectrum of density fluctuations from FIR scattering for bean and oval plasmas.

Acknowledgments

This work was supported by the U.S. Department of Energy under DE-AC05-00OR22725, DE-FG03-97ER54415, DE-FC02-04ER54698, SC-G903402, W-7405-ENG-48, DE-FG02-89ER53297, and DE-FG03-01ER54615.

References

[1] WESSON, J., Plasma Phys. and Control. Fusion **28** (1985) 243.
[2] GIMBLETT, C. , and HASTIE, J., Plasma Phys. Control. Fusion **36** (1994) 1439.
[3] WAELBROECK, F.L., Phys. Fluids B **1** (1989) 499.
[4] ROGERS, B., and SAKHAROV, L., Phys. Plasmas **2** (1995) 3420.
[5] BIKAMP, D., and SATO, T., Phys.Plasmas **4** (1997) 1326.
[6] BUSSAC, N.M., *et al.,* Phys. Rev. Lett. 35 (1975) 1638.
[7] NAGAYAMA, Y., *et al.,* Phys. Rev. Lett. **69** (1992) 2376.